



Nanoscale

RNA-DNA hybrid nanoshapes that self-assemble dependent on ligand binding

Journal:	<i>Nanoscale</i>
Manuscript ID	NR-ART-11-2019-009706.R1
Article Type:	Paper
Date Submitted by the Author:	05-Jan-2020
Complete List of Authors:	Hermann, Thomas; University of California San Diego, Chen, Shi; University of California San Diego, a. Materials Science and Engineering Program

SCHOLARONE™
Manuscripts

ARTICLE

RNA-DNA hybrid nanoshapes that self-assemble dependent on ligand binding†

Shi Chen,^a and Thomas Hermann^{*b,c}Received 00th January 20xx,
Accepted 00th January 20xx

DOI: 10.1039/x0xx00000x

Self-assembly of nucleic acid nanostructures is driven by selective association of oligonucleotide modules through base pairing between complementary sequences. Herein, we report the development of RNA-DNA hybrid nanoshapes that conditionally assemble under the control of an adenosine ligand. The design concept for the nanoshapes relies on ligand-dependent stabilization of DNA aptamers that serve as connectors between marginally stable RNA corner modules. Ligand-dependent RNA-DNA nanoshapes self-assemble in an all-or-nothing process by coupling adenosine binding to the formation of circularly closed structures which are stabilized through continuous base stacking in the resulting polygons. By screening combinations of various DNA aptamer constructs with RNA corner modules for the formation of stable complexes, we identified adenosine-dependent nanosquares whose shape was confirmed by atomic force microscopy. As a proof-of-concept for sensor applications, adenosine-responsive FRET-active nanosquares were obtained by dye conjugation of the DNA aptamer components.

Introduction

Nucleic acid nanotechnology aims at designing and building functional architectures from oligonucleotides which fold and self-assemble through base pairing between complementary sequence segments.¹⁻³ Nanostructures that assemble or respond dependent on the presence of a ligand have been obtained by incorporating aptamer motifs for adaptive recognition. Nucleic acid aptamers fold concurrently with ligand association and provide a conformational transduction mechanism that couples molecular recognition with structure change.⁴ Ligand-responsive molecular devices for cellular delivery and sensing applications have been obtained by adding aptamers to self-assembling DNA and RNA nanostructures.⁵⁻¹¹ In these systems, ligand-dependent functionality is achieved by aptamers serving as a decoration rather than as intrinsic building blocks of the nanostructures.¹²⁻¹⁴ Alternative approaches seek to incorporate aptamers as architectural motifs into origami folds or complex nano-assemblies.¹⁵⁻²⁰ In few instances, synthetic aptaswitches or natural riboswitches have been used directly as discrete modules for self-assembling nanostructures.^{21, 22} While the use of nucleic acid components for nanotechnology applications has been pursued for DNA or RNA largely separately,^{1, 2} or through hybridizing DNA and RNA strands in simple helices,²³⁻²⁵ we have recently introduced

hybrid nanoshapes that self-assemble from combinations of autonomous RNA motifs as architectural joints and discrete DNA building blocks as functional modules.²⁶ The modular architecture of the hybrid nanoshapes lends itself to the incorporation of aptamer building blocks that allow for ligand control over nanostructure assembly and function. Here, we describe the design and development of RNA-DNA hybrid nanoshapes that conditionally assemble under the control of adenosine and its derivatives.

Experimental

Materials

DNA and RNA oligonucleotides, including HPLC purified dye-conjugated oligonucleotides, were purchased from Integrated DNA Technologies. Lyophilized oligonucleotides were rehydrated by dissolving in 10 mM sodium cacodylate buffer, pH 6.5. Adenosine monophosphate disodium salt (CAS 4578-31-8) was purchased from Sigma-Aldrich and adenine hydrochloride (CAS 2922-28-3) from Spectrum Chemical.

RNA-DNA hybrid nanostructure preparation

RNA-DNA hybrid assemblies were prepared by mixing the constituent oligonucleotides at equimolar concentration (100 μ M) with the desired amount of magnesium chloride (to 2 mM or 5 mM final concentration) and adenosine or adenine salt (to 100 μ M). Samples were annealed by heating at 65°C for 5 minutes followed by incubation at 37°C for 10 minutes before cooling in an ice bath for 5 minutes.

Gel electrophoresis

^a Materials Science and Engineering Program, University of California, San Diego, 9500 Gilman Drive, La Jolla, CA 92093, USA

^b Department of Chemistry and Biochemistry, University of California, San Diego, 9500 Gilman Drive, La Jolla, California 92093, USA. E-mail: tch@ucsd.edu

^c Center for Drug Discovery Innovation, University of California, San Diego, 9500 Gilman Drive, La Jolla, CA 92093, USA

†Electronic Supplementary Information (ESI) available. See DOI: 10.1039/x0xx00000x

Polyacrylamide gel electrophoresis was performed on 5% acrylamide/bisacrylamide (19:1) native gel. Gels were run at 220 V, 22 mA for about 1h in 2X MOPS buffer (40 mM 3-morpholinopropane 1-sulfonic acid, 10 mM sodium acetate) and the appropriate magnesium chloride concentration, if desired (2 mM or 5 mM). Visualization of nucleic acid complexes was performed under UV light after ethidium bromide staining.

AFM imaging

Samples for AFM imaging were prepared on freshly cleaved mica which was modified with 50 mM aqueous solution of 1-(3-aminopropyl)-silatrane (APS) by immersing for 30 min followed by rinsing with deionized water and drying in an argon stream.²⁷ Imaging samples were diluted at 4°C in buffer containing 10 mM HEPES, pH 7, and 2 mM magnesium chloride to 0.5–1.5 ng/μL concentration, and deposited onto APS-modified mica for 2 min. After deposition, mica strips were rinsed briefly with ice cold water and dried under flowing argon. AFM images were recorded with a MultiMode AFM Nanoscope IV system (Bruker Instruments) in Tapping Mode with silicon probes RTESPA-300 (Bruker Nano Inc.; resonance frequency ~300 kHz, spring constant ~40 N/m) at a scanning rate of ~2.0 Hz. Image processing was performed with the FemtoScan software package (Advanced Technologies Center).

FRET experiments

Nucleic acid assemblies containing dye-conjugated oligonucleotides were annealed at 200 nM concentration in 10m M HEPES (4-(2-hydroxyethyl)-1-piperazineethanesulfonic acid) buffer, pH 7.0, by the same annealing protocol described above. 95 μL of each sample was then transferred to a 96-well plate and incubated in the dark at room temperature for 1–2 h prior to measurement. FRET measurements were performed on a Spectra Max Gemini XS monochromator plate reader (Molecular Devices) at 22°C by exciting the Cy3 fluorophore at 520 nm and reading the transferred fluorescence as Cy5 emission at 670 nm. An emission cut-off filter was applied at 665 nm.

Results and discussion

Design and discovery of ligand-dependent nanoshapes

Hybrid RNA-DNA nanoshapes are circularly closed nucleic acid structures that form by association between single-stranded regions in bent RNA modules and straight DNA. For the design blueprint of ligand-dependent nanoshapes, we combined a previously discovered RNA corner motif²⁸ with variants of DNA connectors derived from an adenosine/AMP/ATP-binding aptamer whose solution structure in complex with AMP had been determined by NMR spectroscopy (Fig. 1).^{29, 30} Design parameters included the number of base pairs closing the adenosine-binding loop (Fig. 1A, variables *y* and *z*) as well as the length of the single-stranded region for association between RNA and DNA modules (Fig. 1A, variable *x*).

To identify combinations of the RNA corner motif with DNA aptamer connectors that assemble into stable nanostructures,

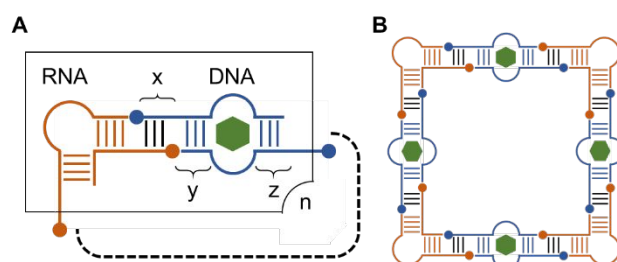


Fig. 1 Design of ligand-dependent RNA-DNA hybrid nanoshapes. (A) A bent RNA motif as architectural joint and a ligand-bound DNA aptamer module connect to form closed RNA-DNA hybrid nanoshapes. A screening library of RNA and DNA components is obtained by choice of the DNA aptamer and length variation of the flanking double-stranded regions (*y*, *z*) as well as the single-stranded overhang (*x*) for hybridization between the building blocks. Ligand is shown as hexagon. (B) Example of an RNA-DNA hybrid nanosquare.

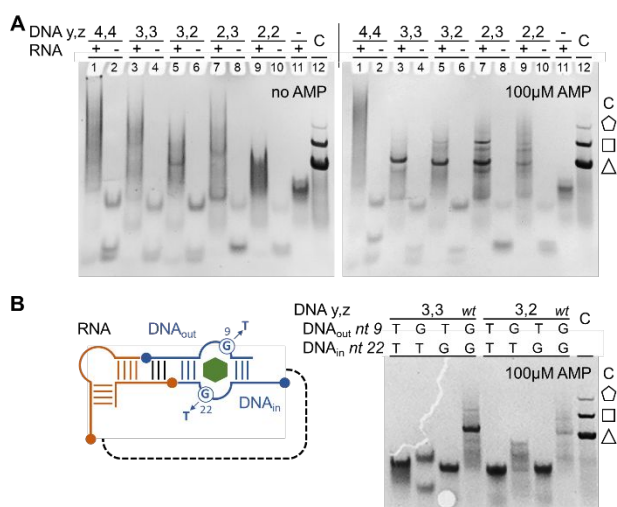


Fig. 2 Discovery of ligand-dependent RNA-DNA hybrid nanoshapes. (A) Screening by native polyacrylamide gel electrophoresis (PAGE) for stable nanoshapes that assemble from an RNA corner motif and variants of an AMP-binding DNA aptamer module in the presence of 2 mM magnesium ions. Stable RNA-DNA hybrid nanoshapes give rise to discrete bands without leaving nucleic acid material retained in the gel pocket. DNA aptamer modules were tested that contain single-stranded overhangs (*x*) of 6 nucleotides and different lengths of the double stranded regions (*y*, *z*) flanking the AMP-binding loop (see Supplementary Figure S1 for sequences). PAGE analysis of the RNA-DNA module combinations was performed on two separate gels, respectively, in the absence and presence of 100 μM AMP ligand. For each aptamer variant, the DNA module was tested by itself and in combination with the RNA corner motif (lanes 1–10). Control lanes show the RNA corner by itself (lane 11) and, as similarly-shaped size markers, hybrid nanoshapes (C, lane 12) that contain the same RNA corner motif connected by a simple double-stranded DNA module of 11 base pairs flanked by 6-nucleotide single-stranded overhangs. Nanoshapes used for the control (C, lane 12) assemble as a mixture of polygons as previously confirmed by atomic force microscopy (AFM). (B) PAGE analysis of nanoshapes that contain mutated DNA aptamer modules carrying single or double base changes (G→T) at positions 9 and 22 of the AMP binding loop which ablate ligand recognition. Mutation at either position prevent formation of the nanoshapes in the presence of AMP. Numbering was adapted from a construct that had been used to determine the solution structure of the aptamer.³⁰ For reference, a control lane is included showing a mixture of polygonal nanoshapes containing a simple DNA helix module as described in panel A.

we intended to use a gel-based screening approach which we previously developed for the discovery of self-assembling hybrid nanoshapes.²⁶ A small library of DNA building blocks was conceived that contained the adenosine-binding loop flanked

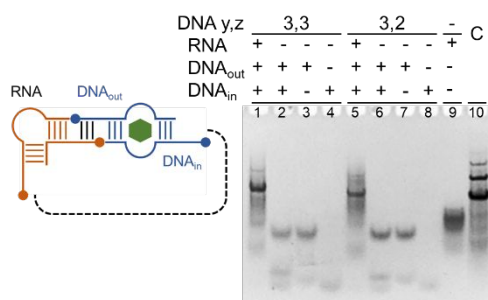


Fig. 3 PAGE analysis of the nucleic acid components that were used to assemble RNA-DNA hybrid nanoshapes containing DNA aptamer modules in the presence of 100 μ M AMP ligand. Aptamer DNA insert variants were tested as individual strands (lanes 3, 4, 7, 8) and as DNA duplex (lanes 2, 6) in comparison with the combination with the RNA corner motif (lanes 1, 5). Analysis of individual DNA strands in combination with the RNA corner motif is shown in ESI Fig. S5[†]. RNA corner by itself is applied in lane 9. Lane 10 (C) shows hybrid nanoshapes that contain the same RNA corner motif connected by a simple double-stranded DNA module of 11 base pairs flanked by 6-nucleotide single-stranded overhangs.

by short base-paired regions of 2-4 nucleotides (ESI Fig. S1[†]). The rationale for these design parameters was that such intrinsically labile aptamer duplexes were to depend on concurrent ligand binding and hybridization with RNA corner modules for robust strand association which, in turn, furnished circularly closed nanoshapes. For connection of the RNA and DNA modules by hybridization, complementary single-stranded sequences of 6 nucleotides were added. In previous studies that established the hybrid RNA-DNA nanoshapes, we found that among a range of 5-8 nucleotide overhangs tested, 6 residues provide an optimal compromise between stability and sensitivity towards geometry changes in the nanoshapes.²¹

Combinations of the RNA corner motif and variants of the DNA aptamer module were screened by native polyacrylamide gel electrophoresis (PAGE) to detect formation of stable nanostructures in the presence of AMP and 2 mM magnesium salt (Fig. 2A). DNA connectors which had the ligand-binding loop bracketed between 3 base pairs on the left ($y = 3$) and 2 or 3 base pairs on the right side ($z = 2-3$), (DNA 3,3 and DNA 3,2), gave rise to a single species of RNA-DNA hybrid complex in the presence of 100 μ M AMP ligand. In the absence of AMP, none of the tested RNA-DNA combinations produced stable assemblies. At a higher magnesium concentration of 5 mM, a slightly increased occurrence of DNA 3,3 and DNA 3,2 assemblies was observed in the absence of AMP, perhaps attributable to stabilization of the RNA corner modules by the divalent ions (ESI Fig. S2[†]); however, the clear distinction of fully stable complexes requiring the ligand remained. Stable nanostructures were also obtained for the combinations of RNA corner and DNA 3,3 or 3,2 aptamer modules in the presence of adenine instead of AMP (ESI Fig. S3[†]), as was expected due to the base-selectivity of the DNA aptamer for adenine and its glycoside derivatives.²⁹ The uncharged nature of the adenine ligand led to complexes migrating slower on native polyacrylamide gel relative to AMP-bound nanostructures (ESI Fig. S3[†]).

Gel electrophoretic characterization of nanoshapes

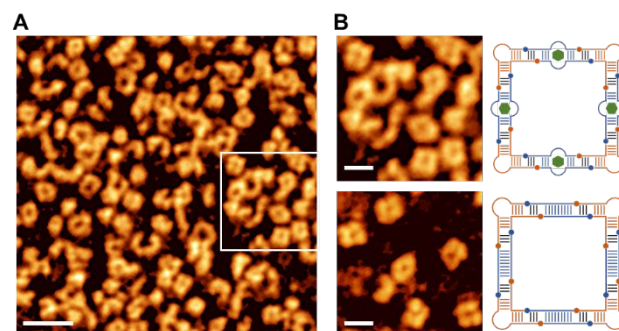


Fig. 4 Atomic force microscopy (AFM) imaging of RNA-DNA hybrid nanoshapes. (A) AFM image of nanoshapes obtained from combination of the RNA corner motif and DNA 3,3 aptamer module in the presence of 100 μ M AMP ligand and 2 mM magnesium salt. Scale bar represents 50 nm. See also ESI Fig. S7AB[†]. (B) Detail view (boxed area in panel A) of square nanoshapes from RNA corner motif and DNA 3,3 aptamer with AMP (top) in comparison to purified nanosquares (bottom) obtained from a nanoshape mixture that assembled from the same RNA corner and a simple double-stranded DNA module. Scale bar represents 20 nm.

Surprisingly, monovalent cations inhibited the formation of the RNA-DNA aptamer nanostructures at 100 mM concentration, with potassium exerting a stronger inhibitory effect than sodium, and affecting the complex including the DNA 3,2 module more significantly than the assembly containing DNA 3,3 (ESI Fig. S4[†]). Inhibition of nanostructure formation by potassium and sodium may be related to their stabilizing effect on an alternative G-quartet structure perhaps involving the guanine-rich DNA aptamer outer strand (ESI Fig. S1[†]).^{29, 31} While the architecture of the AMP-bound aptamer does not contain a G-quartet,³⁰ high concentrations of monovalent ions may sequester such an alternative configuration within one or both of the component DNA strands and thereby prevent their availability to participate in the aptamer-ligand complex.

The design premise for the DNA aptamer modules to gain duplex stability through concurrent association with both AMP ligand and RNA corners was tested by PAGE analysis of the constitutive oligonucleotides (Fig. 3 and ESI Fig. S5[†]). DNA aptamer duplexes did not form in the presence of 100 μ M AMP ligand, suggesting that the nanostructures identified by screening (Fig. 2A) self-assemble in an all-or-nothing process that requires the presence of all components, including RNA corners, DNA aptamer strands and ligand. To unequivocally prove that AMP binding at the aptamer loop is essential for nanoshape formation, DNA connector constructs derived from DNA 3,3 and DNA 3,2 were tested which carried single or double base changes at two key bases involved in ligand binding (Fig. 2B).²⁹ Mutation at any of these positions ablated nanoshape assembly in the presence of AMP or adenine (ESI Fig. S6[†]), thus demonstrating the obligatory requirement for ligand binding at the aptamer loop.

Atomic force microscopy of nanoshapes

Electrophoretic mobility of the complex assemblies formed with the DNA 3,3 and DNA 3,2 aptamer inserts in the presence of AMP was similar to that of previously developed triangle nanoshapes which carried the same RNA corner motif connected by a simple double-stranded DNA module of 11 base

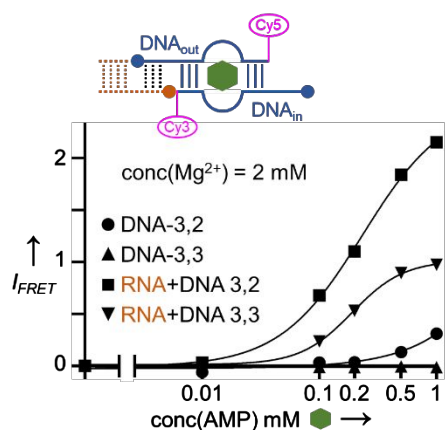


Fig. 5 FRET response in titrations of fluorescently labeled nanoshape component mixtures with AMP ligand in the presence of 2 mM magnesium ions. Mixtures contained DNA aptamer variant strands with the FRET dye pair Cy3/Cy5 attached at the 3' terminus of, respectively, DNA_{in} and DNA_{out} (DNA 3,2 ● and DNA 3,3 ▲), and the same DNA strands combined with the RNA corner motif (RNA+DNA 3,2 ■ and RNA+DNA 3,3 ▼). FRET intensities are plotted as normalized values obtained by subtraction of intensity at [AMP]=0 (first data point) divided by this same number (fractional difference). Each data point is an average of physical triplicates. Error bars of $\pm 1\sigma$ are obscured by the symbols for most data points.

pairs (Fig. 2A).²⁶ Since gel mobility at native conditions depends on both the charge to mass ratio and hydrodynamic radius of the migrating species, which may be affected by a more compact fold of the aptamer inserts along with the presence of charged AMP ligands, PAGE analysis cannot conclusively reveal the composition of the DNA aptamer-containing nucleic acid complexes. To investigate the shape and constitution of the aptamer hybrid nanostructures, atomic force microscopy (AFM) imaging was performed (Fig. 4 and ESI Fig. S7A[†]). AFM analysis of the complexes formed between RNA corner and DNA 3,3 aptamer modules revealed square-shaped nanostructures as the dominant species (Fig. 4A) which were comparable in size to previously described simple RNA-DNA hybrid nanosquares (Fig. 4B)²⁶ but migrated on gel more similar to simple hybrid nanotriangles (Fig. 2A). For the complexes of DNA 3,3 aptamer modules, nanotriangles and larger circularly closed structures were observed by AFM at very low occurrences (ESI Fig. S7B[†]) corresponding to considerably weaker bands for these species on polyacrylamide gel (Fig. 2A).

Nanoshapes as sensors: FRET experiments

To demonstrate proof of concept for the application of ligand-dependent RNA-DNA hybrid nanoshapes as a platform for sensor development, we designed dye-labeled DNA aptamer constructs that create a fluorescent readout upon nanosquare self-assembly (Fig. 5). FRET pair dyes Cy3 and Cy5 were attached at the 3' terminus of the two DNA strands that constitute the aptamer module. Duplex formation during ligand-driven assembly would co-locate the dye pair in close proximity and generate a FRET signal upon excitation of the Cy3 donor dye. To discriminate stabilizing effects of divalent cations from duplex stabilization through ligand binding, we first performed titrations of the fluorescently labeled DNA aptamer strands with magnesium salt in the absence of AMP ligand (ESI Fig. S8[†]). The

pair of DNA strands did not give rise to FRET at magnesium concentrations tested up to 10 mM, which suggests that duplex did not form. However, when RNA corner oligonucleotides were present in the mixture with the DNA strands, a dose-dependent increase of FRET was observed between 2–10 mM magnesium concentration, which suggests that metal-induced folding of RNA corner modules provide a framework to stabilize ligand-free DNA aptamer inserts within RNA-DNA hybrid structures. This hypothesis is consistent with the structure-supporting role identified for magnesium ions that were present at two high-affinity coordination sites in the crystal structure of the RNA corner motif.²⁸ The range of FRET signal increase was nearly identical for the two variants of DNA aptamer inserts tested in RNA hybrid assemblies (DNA 3,2 and DNA 3,3, ESI Fig. S8[†]), which further indicates that magnesium cations exert their stabilizing role on the RNA corner exclusively and without differentially affecting the DNA insert variants. At 2 mM magnesium concentration, the FRET signal from stabilization of RNA-DNA hybrid assemblies in the absence of AMP ligand was minimal (ESI Fig. S9[†]). The small residual FRET signal from marginally stable ligand-free RNA-DNA assemblies was higher for the DNA 3,3 insert than for the DNA 3,2 variant (ESI Fig. S9[†]), likely due to the stabilizing contribution of an additional base pair in the DNA 3,3 construct. Titration of AMP ligand in the presence of 2 mM magnesium induced the formation of hybrid nanoshapes as attested by a significant dose-dependent rise in FRET intensity (Fig. 5, ESI Fig. S9[†]) and in agreement with PAGE analysis (Fig. 2A). The higher background fluorescence observed at 2 mM magnesium for ligand-free assemblies containing the DNA 3,3 variant resulted in an overall reduced dynamic range of FRET signal over the course of the AMP titration compared to assemblies including DNA 3,2. In the absence of RNA corner oligonucleotides, AMP ligand alone was not sufficient to stabilize the DNA aptamer (Fig. 5, ESI Fig. S9[†]). Inhibition of the formation of the RNA-DNA aptamer nanostructures by monovalent cations was demonstrated with the fluorescently labeled DNA aptamer inserts in combination with the RNA corner module (ESI Fig. S10[†]) consistent with PAGE analysis (ESI Fig. S4[†]).

Future applications of the modular RNA-DNA aptamer nanoshapes may exploit the ability to use metal ion concentration for adjusting nanostructure stability coupled to ligand binding. For example, fluorescently labeled nanosquare constructs carrying the DNA 3,2 aptamer inserts were able to discriminate cognate ligands such as AMP and adenine from other nucleobase derivatives such as GMP (ESI Fig. S11[†]).

Conclusions

We designed hybrid nanoshapes that self-assemble from RNA corner modules and DNA aptamer inserts dependent on the concurrent presence of both divalent metal cations and aptamer ligand. Robust assembly of nanoshapes requires ligand binding at the DNA aptamer inserts. RNA-DNA hybrid nanoshapes that include aptamer modules provide a novel general blueprint for the design of stimulus-responsive materials. The modular nature of the hybrid nanoshapes, along

with their exceptional ability to tolerate a wide range of DNA insert topologies²⁶ will open new avenues for the development of smart materials and sensors for diverse analytes.

Conflicts of interest

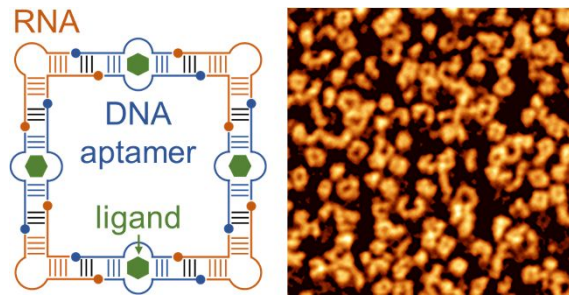
There are no conflicts to declare.

Acknowledgements

We thank A. J. Lushnikov for help with AFM imaging. This work was supported by the National Science Foundation, Chemical Measurement & Imaging Program, grant number CHE CMI 1608287.

References

- N. C. Seeman, C. Mao and H. Yan, *Accounts of Chemical Research*, 2014, **47**, 1643-1644.
- D. Jasinski, F. Haque, D. W. Binzel and P. Guo, *ACS Nano*, 2017, **11**, 1142-1164.
- H. Ohno, S. Akamine and H. Saito, *Current Opinion in Biotechnology*, 2018, **58**, 53-61.
- T. Hermann and D. J. Patel, *Science*, 2000, **287**, 820-825.
- A. Khaled, S. Guo, F. Li and P. Guo, *Nano Letters*, 2005, **5**, 1797-1808.
- D. Shu, Y. Shu, F. Haque, S. Abdelmawla and P. Guo, *Nature Nanotechnology*, 2011, **6**, 658-667.
- S. M. Douglas, I. Bachelet and G. M. Church, *Science*, 2012, **335**, 831-834.
- E. F. Khisamutdinov, D. L. Jasinski, H. Li, K. Zhang, W. Chiu and P. Guo, *Advanced Materials*, 2016, **28**, 10079-10087.
- C. Geary, A. Chworos, E. Verzemnieks, N. R. Voss and L. Jaeger, *Nano Letters*, 2017, **17**, 7095-7101.
- J. M. O'Hara, D. Marashi, S. Morton, L. Jaeger and W. W. Grabow, *Nanomaterials*, 2019, **9**, 378.
- A. Chopra, S. Sagredo, G. Grossi, E. S. Andersen and F. C. Simmel, *Nanomaterials*, 2019, **9**, 507.
- K. A. Afonin, E. Bindewald, A. J. Yaghoubian, N. R. Voss, E. Jacovetty, B. A. Shapiro and L. Jaeger, *Nature Nanotechnology*, 2010, **5**, 676-682.
- Y. Sakai, M. S. Islam, M. Adamiak, S. C. Shiu, J. A. Tanner and J. G. Heddle, *Genes*, 2018, **9**, 571.
- M. Panigaj, M. B. Johnson, W. Ke, J. McMillan, E. A. Goncharova, M. Chandler and K. A. Afonin, *ACS Nano*, 2019, DOI: 10.1021/acsnano.9b06522.
- M. D. E. Jepsen, S. M. Sparvath, T. B. Nielsen, A. H. Langvad, G. Grossi, K. V. Gothelf and E. S. Andersen, *Nature Communications*, 2018, **9**, 18.
- A. Krissanaprasit, C. Key, M. Fergione, K. Froehlich, S. Pontula, M. Hart, P. Carriel, J. Kjems, E. S. Andersen and T. H. LaBean, *Advanced Materials*, 2019, **31**, e1808262.
- H. Pei, L. Liang, G. Yao, J. Li, Q. Huang and C. Fan, *Angewandte Chemie International Ed.*, 2012, **51**, 9020-9024.
- A. Banerjee, D. Bhatia, A. Saminathan, S. Chakraborty, S. Kar and Y. Krishnan, *Angewandte Chemie International Ed.*, 2013, **52**, 6854-6857.
- Z. Liu, C. Tian, J. Yu, Y. Li, W. Jiang and C. Mao, *Journal of the American Chemical Society*, 2015, **137**, 1730-1733.
- W. C. Liao, C. H. Lu, R. Hartmann, F. Wang, Y. S. Sohn, W. J. Parak and I. Willner, *ACS Nano*, 2015, **9**, 9078-9086.
- L. Azema, S. Bonnet-Salomon, M. Endo, Y. Takeuchi, G. Durand, T. Emura, K. Hidaka, E. Dausse, H. Sugiyama and J. J. Toulme, *Nucleic Acids Research*, 2018, **46**, 1052-1058.
- C. Mitchell, J. A. Polanco, L. DeWald, D. Kress, L. Jaeger and W. W. Grabow, *Nucleic Acids Research*, 2019, **47**, 6439-6451.
- J. R. Halman, E. Satterwhite, B. Roark, M. Chandler, M. Viard, A. Ivanina, E. Bindewald, W. K. Kasprzak, M. Panigaj, M. N. Bui, J. S. Lu, J. Miller, E. F. Khisamutdinov, B. A. Shapiro, M. A. Dobrovolskaia and K. A. Afonin, *Nucleic Acids Research*, 2017, **45**, 2210-2220.
- W. Ke, E. Hong, R.F. Saito, M. C. Rangel, J. Wang, M. Viard, M. Richardson, E. F. Khisamutdinov, M. Panigaj, N. V. Dokholyan, R. Chammas, M. A. Dobrovolskaia and K. A. Afonin, *Nucleic Acids Research*, 2019, **47**, 1350-1361.
- P. Zakrevsky, E. Bindewald, H. Humbertson, M. Viard, N. Dorjsuren and B. A. Shapiro, *Nanomaterials*, 2019, **9**, 615.
- A. Monferrer, D. Zhang, A. J. Lushnikov and T. Hermann, *Nature Communications*, 2019, **10**, 608.
- L. S. Shlyakhtenko, A. A. Gall, A. Filonov, Z. Cerovac, A. Lushnikov and Y. L. Lyubchenko, *Ultramicroscopy*, 2003, **97**, 279-287.
- S. M. Dibrov, H. Johnston-Cox, Y. H. Weng and T. Hermann, *Angewandte Chemie International Ed.*, 2007, **46**, 226-229.
- D. E. Huizenga and J. W. Szostak, *Biochemistry*, 1995, **34**, 656-665.
- C. H. Lin and D. J. Patel, *Chemistry & Biology*, 1997, **4**, 817-832.
- C. C. Hardin, A. G. Perry and K. White, *Biopolymers*, 2000, **56**, 147-194.

Table of contents entry:

Composite nanoshapes self-assemble from RNA and DNA modules by coupling ligand binding to the formation of circularly closed structures.